Icarus **157**, 155–172 (2002)
doi:10.1006/icar.2002.6830, available online at http://www.idealibrary.com on IDEAL®

The Flora Family: A Case of the Dynamically Dispersed Collisional Swarm?

D. Nesvorný

Observatoire de la Côte d'Azur, B.P. 4229, 06304 Nice Cedex 4, France; and Department of Space Studies, Southwest Research Institute, 1050 Walnut Street, Suite 426, Boulder, Colorado 80302
E-mail: davidn@boulder.swri.edu

A. Morbidelli

Observatoire de la Côte d'Azur, B.P. 4229, 06304 Nice Cedex 4, France

D. Vokrouhlický

Institute of Astronomy, Charles University, V Holešovičkách 2, 18000 Prague 8, Czech Republic

W. F. Bottke

Department of Space Studies, Southwest Research Institute, 1050 Walnut Street, Suite 426, Boulder, Colorado 80302

and

M. Brož

Institute of Astronomy, Charles University, V Holešovičkách 2, 18000 Prague 8, Czech Republic

Received May 1, 2001; revised December 21, 2001

Asteroid families are believed to originate by catastrophic disruptions of large asteroids. They are nowadays identified as clusters in the proper orbital elements space. The proper elements are analytically defined as constants of motion of a suitably simplified dynamical system. Indeed, they are generally nearly constant on a 10^7–10^8-year time scale. Over longer time intervals, however, they may significantly change, reflecting the accumulation of the tiny nonperiodic evolutions provided by chaos and nonconservative forces. The most important effects leading to a change of the proper orbital elements are (i) the chaotic diffusion in narrow mean motion resonances, (ii) the Yarkovsky nongravitational force, and (iii) the gravitational impulses received at close approaches with large asteroids. A natural question then arises: How are the size and shape of an asteroid family modified due to evolution of the proper orbital elements of its members over the family age? In this paper, we concentrate on the dynamical dispersion of the proper eccentricity and inclination, which occurs due to (i), but with the help of (ii) and (iii). We choose the Flora family as a model case because it is unusually dispersed in eccentricity and inclination and, being located in the inner main belt, is intersected by a large number of effective mean motion resonances with Mars and Jupiter. Our results suggest that the Flora family dynamically disperses on a few 10^8-year time scale and that its age may be significantly less than 10^9 years. We discuss the possibility that the parent bodies of the Flora family and of the ordinary L chondrite meteorites are the same object. In a broader sense, this work suggests that the common belief that the present asteroid families are simple images of their primordial dynamical structure should be revised.

Key Words: **asteroids; dynamics; meteorites; resonances.**

1. INTRODUCTION

The asteroid families are groups of asteroids identified on the basis of the proper orbital elements (Zappalà *et al*. 1994). They are remnants of collisional disruption of large parent bodies which occurred hundreds of Myr to a few Gyr ago. The proper elements are analytically defined as constants of motion of a suitably simplified dynamical system, achieved from the original dynamical system using the classical tools of the "normal form" theory (Milani and Knežević 1990; see also chapter 8 of Morbidelli 2002). In practice, if the real dynamics is regular (i.e., quasi-periodic), the analytically defined proper elements show only very small oscillations around a mean value that stays constant with time (Knežević *et al*. 1995). However, if the motion is chaotic, the mean value of the proper elements can drift in time, at a rate that depends on the properties of the chaotic motion (Milani and Farinella 1994). The slow drift of proper elements is called *chaotic diffusion*.

0019-1035/02 $35.00

Most of the asteroids do not exhibit any macroscopic chaotic diffusion on a 10^7–10^8 yr time scale (Milani and Farinella 1994, Knežević *et al*. 1995). For this reason, it has been assumed in many works by extrapolation that the proper elements are constant in time and therefore that asteroid families are dynamically "frozen" in proper elements space (Zappalà *et al*. 1996, Cellino *et al*. 1999, etc.). With this assumption, the dispersion of proper elements of family members has been related to the ejection velocities field of the fragments relative to the parent body. An open problem is that the resulting ejection velocities are much larger (Pisani *et al*. 1999) than those predicted by hydrocode simulations and laboratory experiments (Love and Ahrens 1996, Benz and Asphaug 1999, Fujiwara *et al*. 1989, Martelli *et al*. 1994). Moreover, certain asymmetries of asteroid families cannot be explained. We provide more detail on this in Section 2.

The assumption that the proper elements are constant on time scales comparable to family ages (a few billion years; Marzari *et al*. 1999) has not yet been explicitly demonstrated, as the ages are one to two orders of magnitude longer than the time scale on which the stability of proper elements has been tested. In fact, if we monitor the dynamics on longer and longer time scales, the number of resonances that induce macroscopic chaotic diffusion increases, and consequently the number of asteroids whose proper elements are essentially constant is reduced. This is particularly true in the outer asteroid belt (Murray and Holman 1997) and, if the perturbations exerted by the terrestrial planets are taken into account, the inner asteroid belt (Migliorini *et al*. 1998, Morbidelli and Nesvorný 1999). Moreover, we will see (in Section 5) that if some semimajor axis mobility of asteroids is taken into account, the phenomenon of macroscopic chaotic diffusion becomes general, because virtually any asteroid must spend some appreciable time in a chaotic resonance.

These results lead to the following questions: *What is the effect of the chaotic diffusion on the asteroid families? Could chaotic diffusion explain the large dispersion of family members and the observed asymmetries, without the need to invoke huge and anomalous ejection velocity fields?* Answering these questions is the primary motivation of this paper. In the "fairy tale" that we have in mind, a family loses its fastest diffusing members while dispersing as a whole due to dynamical diffusion driven by the background chaos. Of course, the relevance and time scale of this process need to be quantified. Evidence that some family members can significantly evolve and escape from a family has been found by Milani and Farinella (1994). Indeed, (490) Veritas—the largest member of the Veritas family—can dynamically evolve from its current location to outside the family limits on a <100 Myr time scale.

Numerical simulations (Morbidelli and Nesvorný 1999) and semianalytical estimates (Murray and Holman 1997) showed that the speed of the chaotic diffusion taking place in a mean motion resonance is, in general, an increasing function of resonance width. Wide mean motion resonances usually act fast and lift eccentricities above planet-crossing limits in a few million years, at most (Gladman *et al*. 1997). The escape of objects from these resonances leaves easily recognizable gaps (e.g., Kirkwood gaps) in the present asteroid belt. On the contrary, most of the *very* narrow resonances ($<10^{-5}$ AU), although being densely located all over the belt, do not modify e and i over astronomically relevant time scales (Murray and Holman 1997).

The interesting case from the point of view of orbital diffusion is that of the mean motion resonances of intermediate sizes ($\sim 5 \times 10^{-2} - 10^{-4}$ AU), which change e and i of asteroidal orbits on typical time scales of 10^8–10^9 years. A large but poorly quantified number of asteroids are located in these narrow resonances (Nesvorný and Morbidelli 1998). The mechanism forcing asteroidal e and i values to drift is not fully understood, but presumably it is a consequence of the multiplet structure that these resonances have when one takes into account the eccentricity, the inclination, and the secular precession of planetary orbits (Murray and Holman 1997, Nesvorný and Morbidelli 1999). Unlike proper e and i, a single narrow mean motion resonance does not have any macroscopic effect on the proper semimajor axis a of a resonant body.

There are at least two phenomena, however, which can significantly change the semimajor axis of small bodies. The first one is the gravitational effect of large asteroids like (1) Ceres, (2) Pallas, and (4) Vesta. Nearly all bodies in the asteroid belt cross the orbits of these large asteroids and may potentially approach them from a small distance. If the mutual encounter velocity is low, the trajectory of a small body is gravitationally deflected by the larger asteroid, with consequent change of the heliocentric orbital elements. While probabilities and typical mutual velocities of such encounters are well understood (Farinella and Davis 1992, Bottke *et al*. 1994), the resulting longterm evolution of the orbital elements is less known (J. C. Williams, Personal Communication, 1992; see Milani and Knežević 1992). Vokrouhlický *et al*. (2001) have shown that the occasional close encounters with (1) Ceres may result in 0.00075 AU jumps in the semimajor axis.

The second phenomenon moving the semimajor axis of (preferentially smaller) asteroids is the Yarkovsky effect (Öpik 1951). This thermal reemission effect has been the subject of many recent works in which the semimajor axis mobility and its dependence on a variety of physical and dynamical parameters has been computed (Rubincam 1995, 1998, Vokrouhlický 1998a,b, 1999, Vokrouhlický and Farinella 1998, 1999, Hartmann *et al*. 1999, Bottke *et al*. 2000, Spitale and Greenberg 2001).

To realistically model the dynamical evolution of an asteroid family, we have to account for semimajor axis mobility. The histories of asteroidal orbits then become complex because the semimajor axes change, allowing the bodies to move relative to the mean motion resonances, either passing through or being temporarily captured in them. What counts is the time that each body spends on a resonant orbit, because this determines the magnitude of the changes of proper e and i due to resonant-driven chaotic diffusion. The probability of capture

and time spent on a resonant orbit are very poorly understood (classical adiabatic capture theory—Henrard 1982—does not apply in these cases), and in the absence of theoretical arguments we resort to numerical simulations.

Although some of our simulations incorporate the phenomenon of semimajor axis mobility, in this paper we focus only on the resulting dispersion of asteroid families in proper e and i. The dispersion of families in proper semimajor axis will be studied in another paper. We take as a model case the Flora family, because it is unusually dispersed in proper e and i, and being located in the inner main belt, it is intersected by many mean motion resonances with Mars and Jupiter. The Flora family's structure is difficult to interpret as a breakup of a single body under the usual assumption that the postbreakup proper elements have been preserved and thus serves as a nice example of a possibly dynamically evolved family. Our goal is not to exclude other scenarios on Flora family origin (multiple breakup and cratering events, or a superposition of several smaller and distinct groupings; see Cellino and Zappalà 1993 for discussion) but rather to show the trend evolution of size and shape of asteroid families over time scales that largely exceed those for which the conservation of proper elements has been verified.

The dynamical and physical properties of the Flora family are described in Section 2. In a series of numerical simulations, we explore the effect on the Flora family orbital distribution of resonances alone (Section 3), close approaches to the most massive asteroids (Appendix), and the interplay between Yarkovsky and resonant affects (Section 4). In Section 5, assuming a scenario of single breakup, we then discuss the plausible age of the Flora family (estimated from the time needed for reaching the present family size by dynamical dispersion). In Section 6—the most speculative part of the paper—we also discuss the possible relation between the Flora family and the ordinary L chondrite meteorites.

2. PRELIMINARIES ON THE FLORA FAMILY

The inner zone of the asteroid belt is characterized by the presence of three populous clans (named Flora, Nysa, and Vesta in Zappalà *et al*. 1994). The largest among them is associated with (8) Flora. It accounts for 15–20% of the main belt asteroids with $2.1 < a < 2.5$ AU. The Flora family[1] is a large but shallow grouping (Zappalà *et al*. 1994) of S-type asteroids with a steep size distribution, which suggests a collisional origin (Cellino *et al*. 1991). The orbital distribution of the Flora family in the proper elements space (Fig. 1) does not allow reconstruction of the velocity field of ejecta assuming a roughly isotropic single breakup event (Cellino and Zappalà 1993). Indeed, assuming an isotropic breakup at the current family center, the velocities needed to reproduce the dispersions in e ($\sim$0.025) and i ($\sim 2^\circ$) are a factor of 2 and 3 larger, respectively, than the velocities needed to reproduce the family dispersion in a ($\sim$0.06 AU). Similar ratios are also obtained if velocities are calculated with respect to the (8) Flora, assuming its current proper a, e, i to characterize the parent body orbit just before the breakup.[2]

Other questions are raised by the magnitude of the family dispersion in the proper elements space. To reproduce the Flora family dispersion with respect to proper semimajor axis, multikilometer bodies with relative velocities at infinity (V_∞) up to 400 m/s must have been ejected from the disruption site. The initial ejection velocity (V_{ej}) of these bodies may be calculated from $V_{ej}^2 = V_{esc}^2 + V_\infty^2$, where V_{esc} is the "effective" escape velocity.[3]

If the dispersion of the Flora family was created by a single breakup, the ejection velocities of most multikilometer fragments must have been several 100 m/s. Such a scenario is inconsistent with the results of hydrocode simulations (Love and Ahrens 1996, Benz and Asphaug 1999), which otherwise correctly predict the ejection fields and size distributions of the collisional breakups obtained in laboratory experiments (Fujiwara *et al*. 1989, Martelli *et al*. 1994) and those in underground nuclear explosions (Melosh 1989). The hydrocode experiments suggest either (i) most fragments were launched at much smaller velocities or (ii) the deposited energy needed to reproduce such velocities should have led to a fragmentation of the parent body into tiny, unobservable pieces. In fact, this puzzling discrepancy has been used to argue that hydrocodes are unreliable tools for modeling large impact events.

[1] Although other terminology is sometimes used, e.g., Flora "clan" (Zappalà *et al*. 1994), to indicate that the grouping associated with (8) Flora has a complex structure, we adopt here the term "Flora family" used in other recent works (e.g., Cellino *et al*. 1999, Michel *et al*. 2001).

[2] This result was obtained from the Gauss equations. Assuming an isotropic ejection field, fragments resulting from a breakup of the parent body with $a_{\rm PB}$, $e_{\rm PB}$, $i_{\rm PB}$ would be distributed within an ellipsoid in a, e, i centered at $a_{\rm PB}, e_{\rm PB}, i_{\rm PB}$, whose shape and orientation are determined by f and ω (Morbidelli *et al*. 1995), where f and ω are the true anomaly and perihelion argument of the parent body at the time of the breakup. These angles are unknown. Consequently, in order to estimate the magnitude of the ejection velocities from the current family dispersion in a, e, i, certain assumptions must be made for values of f and ω. We choose these angles ($f = 90^\circ$ and $f + \omega = 0^\circ$) in order to derive a *conservative* estimate of the velocities needed to reproduce the observed inclination dispersion of the Flora family. If f or ω were different from the chosen values, then either (i) the cloud of fragments resulting from the isotropic breakup would be diagonal in proper (a, e) space (not observed) or (ii) the velocities suggested by the observed inclination dispersion should have been even larger than those calculated above (Morbidelli *et al*. 1995).

[3] Compensating for collective effects in the cloud of dispersing fragments, $V_{esc}^2 = 1.64 \times GM/R$, where GM is the product of the gravitational constant and the parent body mass, and R is the parent body radius (Petit and Farinella 1993). (8) Flora is about 68 km in radius and 3.3×10^{21} g in mass (assuming 2.5 g/cm^3 density typical for the S-type asteroids). Tanga *et al*. (1999) estimated that the parent body of the Flora family had a mass some 1.75 times larger than that of (8) Flora; consequently, $V_{esc} \approx 100$ m/s.

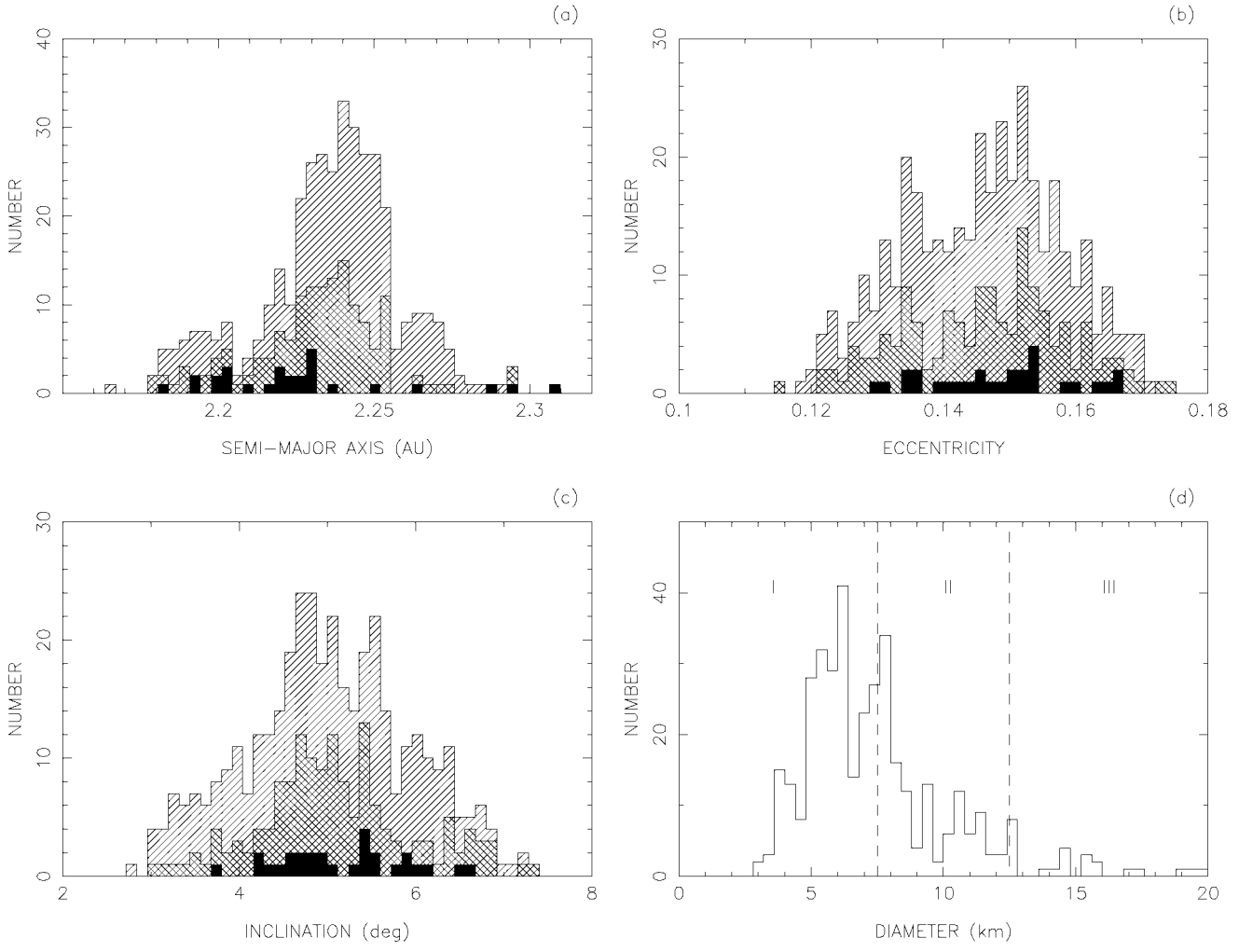

FIG. 1. Histograms of the orbital (a)–(c) and size distributions (d) of the Flora family. The number of asteroids per 1/50 of the x-axis range is shown. The different area fillings in (a), (b), and (c) show the space distribution for different size ranges. We consider three diameter ranges: (I) 0–7.5 km, (II) 7.5–12.5 km, and (III) >12.5 km.

Recently, the breakup of a parent body of the Flora family has been modeled by Michel *et al*. (2001) using a hybrid, hydrocode&N-body code. This work confirmed a large discrepancy between the model-generated small orbital dispersion of the observable (multikilometer) fragments and the much larger dispersion of the currently observed Flora family. This contradiction between the experimental and observational data is relevant to many other asteroid families as well. Michel *et al*. (2001) convincingly showed that the Eunomia and Koronis families' orbital distributions most likely do not reflect the primordial ejection velocities.

Alternatively, to solve the above paradox in the case of the Flora family, some authors discussed the possibility that an ad-hoc sequence of multiple catastrophic (either independent or secondary) events following the primary breakup has created the present family dispersion (Cellino and Zappalà 1993). Here we explore another possibility, which is the effect of chaotic diffusion in dispersing the originally more tightly clustered collision fragments.

3. EVOLUTION OF THE FLORA FAMILY DUE TO RESONANCES

Our list of the Flora family members contains 819 asteroids identified by Zappalà *et al*. (1994). For the purpose of this work, we have selected all *numbered* asteroids, 385 in all,[4] from the list. Such bodies were observed during several oppositions and have well-determined orbits. The orbital elements of the selected objects were obtained from the Asteroid Orbital Elements Database of the Lowell Observatory (ftp://ftp.lowell.edu/

[4] This number refers to all numbered Flora family members identified by the end of 1997.

pub/elgb/astorb.html—Bowell *et al.* 1994). The orbital elements of the planets were obtained from the JPL DE405 ephemeris (http://ssd.jpl.nasa.gov/eph_info.html) and were rotated to the ecliptic reference frame. The asteroids were assumed to be massless test particles (which do not interact between themselves) evolving solely under the gravitational influence of the Sun and seven planets (Venus to Neptune). We used the swift_rmvs3 integration routine of Levison and Duncan (1994) (based on the symplectic scheme of Wisdom and Holman 1991) and a 15-day time step. The integration covered 130 Myr. Three bodies were removed before the end of the integration because they impacted the Sun.

We have computed for each asteroid numerically defined proper elements and their evolution over the integration time span. This has been done by a procedure identical to the one used by Morbidelli and Nesvorný (1999). (Eq. 1): the orbital elements have been numerically averaged over a running window of 10 Myr in size. For our purpose, we have computed proper elements every 10^5 years. We have checked that the 10-Myr averaging window completely removes high frequencies so that the use of a low-pass filter (producing a separate datafile in our run) was unnecessary.

These numerically defined proper elements are different from the analytically defined proper elements discussed in the Introduction, as they are in fact simply *averaged elements* over a very long time span. However, they share with the analytic proper elements the property of being constant with time for regular orbits and changing more or less slowly with time for chaotic orbits. For this reason, we call them *proper* as well. In particular, they are as useful as analytic proper elements to detect chaotic diffusion: if the numerical proper elements change with time in a diffusive manner, the analytic proper elements will also change, and vice versa.

To illustrate the result of our integration, we show in Fig. 2 the evolution of the proper semimajor axis, eccentricity, and inclination of the integrated bodies. In Fig. 2, red dots refer to the bodies when they are on Mars-crossing orbits, namely when their osculating perihelion distance becomes smaller than 1.665 AU. Blue dots refer to bodies with larger perihelion distances. Each body leaves a trace in the proper elements space corresponding to its orbital history on 120 Myr (i.e., 10 Myr less than the integration time span—one loses 10 Myr of the orbital history by the averaging procedure). The two-body mean motion resonances with Mars (light blue) and Jupiter (green) are shown in the background. In Fig. 2a, two lines per resonance are shown, which delimit the resonance width, the latter depending on the eccentricity. In Fig. 2b, the resonance widths have been computed for $e = 0.145$. In addition to the two-body mean motion resonances, there are many (not shown) three-body resonances with Mars and Jupiter located in the semimajor axis range of Fig. 2 (Morbidelli and Nesvorný 1999).

Only a few bodies appear to have regular dynamics (those whose total evolution results in a very short segment). The vast majority exhibits macroscopic diffusion in proper eccentricity and inclination.[5] Until the Mars-crossing status is reached, the proper semimajor axis is basically constant for most bodies. This occurs because the bodies can only diffuse in eccentricity and inclination while staying in the same mean motion resonance or alternating between closely located resonances. The main diffusion track at 2.255 AU is related to the 7/2 mean motion resonance with Jupiter and the 5/9 mean motion resonance with Mars (Morbidelli and Nesvorný 1999). In the Mars-crossing regime, conversely, the bodies start to random-walk in semimajor axis, roughly following a curve of invariant Tisserand parameter with respect to Mars. The change of the semimajor axis is moderate for shallow Mars-crossers and much bigger for deep Mars-crossers.

To characterize the family dispersion we compute the standard deviation at time t,

$$\sigma_1(x;t) = \sqrt{\frac{\sum_j [x_j(t) - \langle x \rangle]^2}{N-1}}\ , \qquad (1)$$

where x stands for proper a, e, or i, and $\langle x \rangle$ is the average over N considered bodies. The standard deviations at time t are computed from the $N(t)$ bodies which are on non-Mars-crossing orbits at time t, their proper elements being computed as the average over the time interval $[t, t + 10$ Myr$]$. In total, we exclude 13 bodies which evolved to Mars-crossing orbits within 130 Myr; the proper elements of these bodies evolve fast and we assume that they would not be recognizable as family members after reaching the Mars-crossing status. From this we can grossly infer that dynamical diffusion causes the Flora family to lose some $13/(385 \times 1.3)$, $\sim$3%, of its members per 10^8 years to the Mars-crossing region. This value does not seem like much, but extrapolating this number over the family age (probably at least a few 10^8 years) implies that $>$10% of the original fragments have been eliminated. This dynamical loss mechanism, together with collisional grinding (Marzari *et al.* 1995, 1999), contributes to the gradual depletion of the Flora family. It is plausible that collisional and dynamical erosion over a long time span eventually lead to a situation where the family is no longer recognizable. Finally, the production rate of planet-crossers by the Flora family is an important fraction of the total production rate of multikilometer objects from the inner asteroid belt (Morbidelli and Nesvorný 1999).

The quantities $\sigma_1(e)$ and $\sigma_1(i)$ grow by 5–10% on 120 Myr (Fig. 3). While $\sigma_1(e)$ rapidly increases during the first 15 Myr and then slows down (with large oscillations), $\sigma_1(i)$ evolves smoothly, growing almost monotonically with time. The rate of these increases is rather surprising; if we extrapolated this trend into the past, the Flora family would shrink to a much

[5] We checked that the periodic oscillations of e and i caused by the secular resonances present near the Flora region (mainly $g - g_6$ and $2(g - g_6) + s - s_6$, g, s, g_6, s_6 being secular frequencies in usual notation—Milani and Knežević 1994) do not significantly contribute to the evolution tracks seen in Fig. 2.

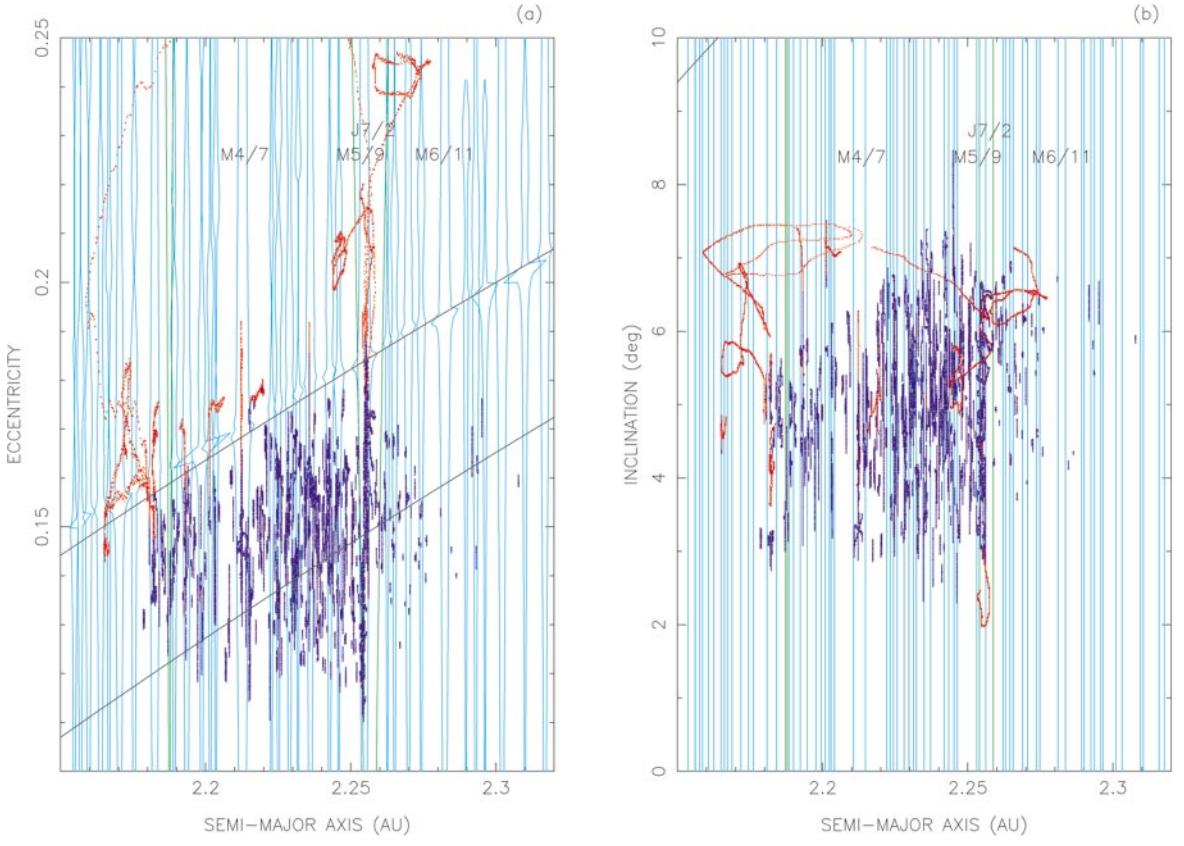
(a)
(b)
M4/7
J7/2
M5/9
M6/11
ECCENTRICITY
INCLINATION (deg)
SEMI−MAJOR AXIS (AU)
0.15
0.2
0.25
0
2
4
6
8
10
2.2
2.25
2.3

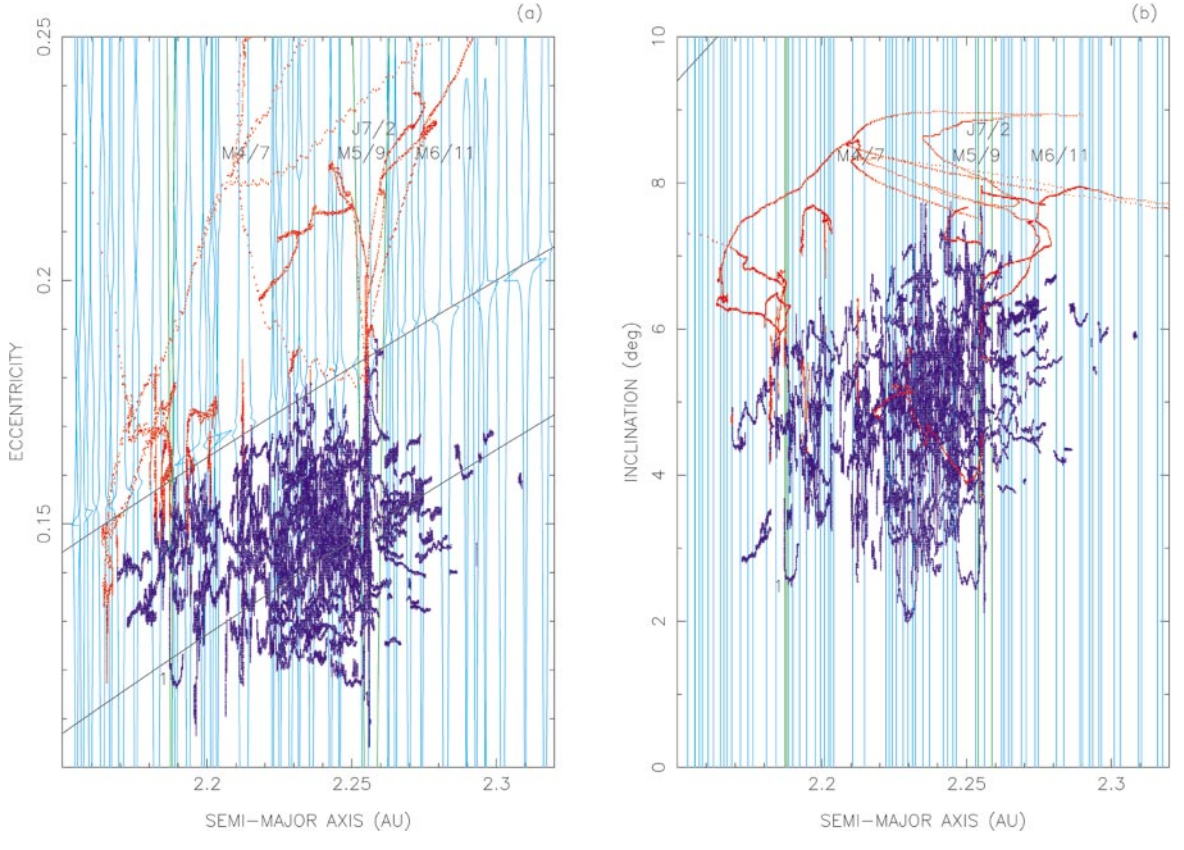
(a)
(b)
M4/7
J7/2
M5/9
M6/11
ECCENTRICITY
INCLINATION (deg)
SEMI−MAJOR AXIS (AU)
0.15
0.2
0.25
0
2
4
6
8
10
2.2
2.25
2.3

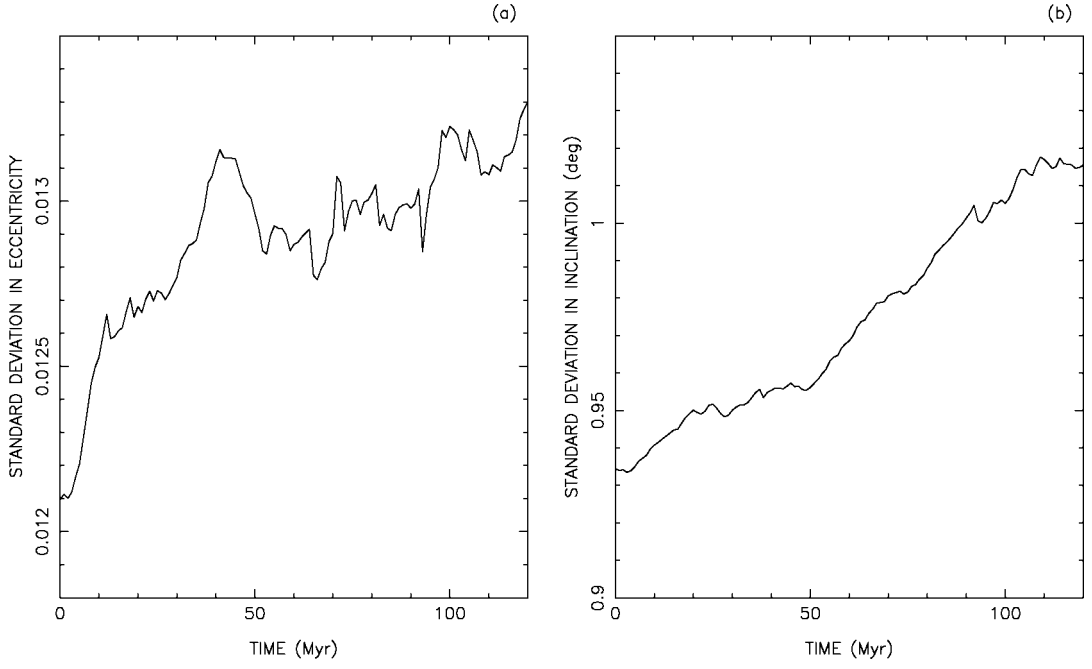

FIG. 3. The standard deviations $\sigma_1(e)$ (a) and $\sigma_1(i)$ (b) computed from Eq. (1). Over the time span covered by the simulation, $\sigma_1(e)$ and $\sigma_1(i)$ increase by 10% and 9%, respectively, with respect to their initial values. Note, however, that the initial trend seen in (a) when $\sigma_1(e)$ sharply increases may result from having neglected the semimajor axis mobility in the model, thus effectively "fixing" the initially resonant bodies in resonances for the whole integration time span. If linear trends were fit to the evolutions, the inferred $\sigma_1(e)$ and $\sigma_1(i)$ changes would be more moderate.

smaller size than its current one in only about 10^8 years. This result indicates that the Flora family may be a relatively young grouping compared with the inferred ages of many other asteroid families (e.g., the Koronis family is believed to be >1 Gyr old; Greenberg *et al.* 1996).

Before discussing this age issue in more detail, however, we must account for the fact that the real dynamics of asteroids is more complex than that simulated here. We must account for the interplay between mean motion resonances and semimajor axis mobility, caused by encounters with large asteroids and by the Yarkovsky effect. The semimajor axis mobility is important in this situation because the diffusion process discussed above is bimodal: the bodies which are not in effective resonances do not evolve much (the most frequent case for $a > 2.26$ AU bodies), while the others stay in fast diffusion tracks for the whole integration and evolve very far from their initial positions. Consequently, without the semimajor axis mobility, we are unable to reproduce the current family starting from a more concentrated cluster since it would create a sort of "bimodal" distribution—peaked at the family center in e and i with large convex tails on both sides. The shape of the real family in e and i (Figs. 1b and 1c) is different.

Our tests show that the effect of encounters with large asteroids such as (1) Ceres, (2) Pallas, and (4) Vesta on the Flora family members is not large (see Appendix). We compute by direct numerical integrations that a typical Flora family member would evolve by $\sim 10^{-3}$ AU on 100 Myr, mainly due to the encounters with (1) Ceres. Since the inner belt is densely populated by mean motion resonances, changes by a few times 10^{-3} AU are enough to deliver some family members to resonances, effectively dispersing the family in e and i. Compared to the Yarkovsky drift values (see below), however, the effect of close encounters with large asteroids is negligible for the Flora members smaller than 10–20 km in diameter. As we are

FIG. 2. The evolution of (a) the proper semimajor axis vs proper eccentricity and (b) the proper semimajor axis vs proper inclination for 385 numbered Flora family members (deep blue and red). Regular bodies appear as a dot, while chaotic bodies drift, leaving a trace. The red color distinguishes the evolution of bodies when they are on Mars-crossing orbits. The two black curves in (a) denote proper perihelion distances equal to 1.94 and 1.84 AU. A firm threshold of the Mars-crossing status cannot be defined with respect to proper perihelion distance because it depends on the secular oscillations of the eccentricity. Note, however, that all bodies with perihelion distance less than 1.84 AU became Mars-crossers. The light blue and green lines denote the mean motion resonances with Mars and Jupiter, respectively, some of which are labeled (J7/2 denotes the 7/2 resonance with Jupiter; M4/7, M5/9, and M6/11 denote the resonances with Mars). Two lines per resonance are shown delimiting its size depending on eccentricity (a). In (b), the resonances were computed for $e = 0.145$.

FIG. 4. The same as Fig. 2 but for the run with the Yarkovsky force. See text for details. A case of a body captured in a tiny mean motion resonance is denoted by "1."

mainly interested in the global orbital dispersion of the Flora family—dominated by small members ($D < 10$ km)—we may safely neglect the gravitational effect of large asteroids in the model and account solely for the Yarkovsky force.

4. EVOLUTION OF THE FLORA FAMILY DUE TO RESONANCES AND THE YARKOVSKY EFFECT

The Yarkovsky effect mainly acts on the semimajor axis. The physics of this effect is in the partial absorption of the solar radiation at the body's surface and its reemission in the infrared band (e.g., Burns *et al*. 1979). The thermal radiation from the hottest parts of the surface carries away more linear momentum than that from the coldest parts, and the overall imbalance of the reemission process results in a recoil force. The secular mobility of the semimajor axis due to this force depends on a variety of physical and dynamical parameters, such as thermal constants, rotation speed, obliquity, and orbital geometry. We detail our choice of parameters in the following.

The Yarkovsky-driven semimajor axis mobility is basically negligible for 50-km and larger diameter asteroids. At large sizes, it scales inversely with a body's mean diameter, so for a typical 10-km diameter asteroid near 2.25 AU, the average semimajor axis drift is on the order of 0.01 AU over 1 Gyr, while for a 1-km asteroid it accounts for approximately 0.04 AU over its estimated collisional lifetime of ∼400 Myr (Farinella and Vokrouhlický 1999), assuming reasonable values for the surface thermal conductivities and rotation rates and averaging over a sample of bodies having random spin axis orientations.

The diurnal variant of the Yarkovsky effect dominates over the seasonal effect for multikilometer asteroids whose surfaces are covered by regolith (Farinella *et al*. 1998). The magnitude and orientation of the diurnal semimajor drift depends on the obliquity (ε—the angle between the normal to the orbital plane and the object's spin axis). A roughly spherical, progradely rotating object drifts to larger a, while a similar but retrogradely rotating object drifts to smaller a. The drift is largest for 0 and 180° obliquities. For $\varepsilon \sim 90°$, where the diurnal drift vanishes, the seasonal effect takes over. The seasonal effect grows in importance for bodies having high thermal conductivity surfaces.

Independently of the body's spin, the seasonal effect decreases the semimajor axis. The asteroidal obliquities are usually unknown but believed to be randomly distributed, so that the expected overall statistical trend of an ensemble of initially localized orbits is their dispersion in semimajor axis, with a minor average displacement toward the Sun due to the seasonal effect (Bottke *et al*. 2000).

There is a qualitative difference between the semimajor axis mobility driven by the gravitational perturbations of massive asteroids and that driven by the Yarkovsky effect. While the proper semimajor axis jumps more or less randomly by close encounters, so that the resulting process is close to a random walk, the Yarkovsky force effects the standard deviation of the semimajor axis distribution of a cluster of bodies in a more complex way. Once an asteroid is placed in the main belt, it starts to migrate, depending on its spin axis orientations and physical properties, outwards (if the diurnal effect dominates and $\varepsilon < 90°$) or inwards (if $\varepsilon > 90°$ or the seasonal effect dominates). The migration speed and direction are fixed until the object has its spin axis reoriented by an impact (Farinella *et al*. 1998). Consequently, the standard deviation computed over an ensemble of bodies (Eq. 1) is by pieces a *linear* function of time with the slope discontinuities at every reorientation event. Initially, $\sigma_1(a)$ must be almost stationary because, assuming random spin axes, there is statistically an equal number of bodies migrating outwards and inwards regardless of the semimajor axis interval. Only later, when a significant number of migrating bodies cross the center of the ensemble, does $\sigma_1(a)$ start to grow. This is because most bodies with semimajor axes smaller than that of the center migrate to smaller semimajor axes, while most bodies with semimajor axes larger than that of the center migrate to larger semimajor axes. Before reorientations become important, the linear growth of $\sigma_1(a)$ may theoretically become as fast as the average migration speed computed over individual bodies.

The time needed for a sizable reorientation of the spin axis of an asteroid grows with its size. It is estimated (Farinella and Vokrouhlický 1999) that the characteristic time scale for the reorientation is $\tau_{\rm REO} \approx 10.6\sqrt{D}$ (in Myr), where D is the asteroid's diameter in meters. This shows that for the range of sizes of the numbered Flora family members, we need not account for spin axis reorientations in the numerical simulation because these are rare over 10^8 years. In later stages, the linear growth of $\sigma_1(a)$ must decelerate when spins get reoriented and the semimajor axis drift changes direction. Eventually, $\sigma_1(a)$ dependence on time basically flattens by collisional breakups of large bodies which tend to generate many fragments close to the family's center.

From a quantitative point of view, we estimate that the Yarkovsky effect produces a larger mobility than do the gravitational perturbations produced by (1) Ceres for asteroidal sizes up to a few tens of kilometers in diameter. As our integrations do not cover time intervals longer than 10^8 years and most members of the Flora family have diameters less than 20 km, we can neglect the perturbations of large asteroids for now and concentrate solely on asteroid mobility via the Yarkovsky effect.

We have numerically integrated 385 numbered Flora family members (the same objects as in Section 3) accounting for the gravitational perturbations of seven planets (Venus to Neptune) and for the Yarkovsky effect. We used the integration package swift_rmvs3, which was modified by M. Brož in order to account for the Yarkovsky force. Both diurnal and seasonal variants of the effect were included in the linearized approximation as described by Vokrouhlický (1998a) and Vokrouhlický and Farinella (1999). The code was verified against the analytic predictions. Vokrouhlický and Farinella (1999), and similarly Spitale and Greenberg (2001), showed that the linearized modeling of the Yarkovsky effect yields reasonably good results (given other sources of uncertainty) for the semimajor axis drifts if the

orbital eccentricity is small enough ($\lesssim$0.5). This is satisfactory for our simulations, where bodies spent most of their dynamical evolution in the low-eccentricity state.

The initial orbital elements of the asteroids and planets were the same as in the experiment of Section 3. In addition, we had to decide the values of several parameters characterizing the Yarkovsky force. Asteroids were assigned a random spin axis orientation. The rotation period was chosen according to a Maxwellian distribution peaked at 8 h, with truncation at minimal and maximal periods of 4 and 12 h, respectively. These values are consistent with observations of the main belt asteroids (Binzel *et al*. 1989). The bulk density was assumed to be 2.5 g/cm^3, which is consistent with recent determinations of mean bulk densities of S-type asteroids (243) Ida, (433) Gaspra, and (433) Eros from space missions (Thomas *et al*. 1996, Yeomans *et al*. 2000). The assumed surface density, 1.5 g/cm^3, was derived from the currently prevailing belief that asteroidal surfaces are covered by regolith (Veverka *et al*. 2001). To compute the asteroids' sizes, we used the IRAS albedo when available and assumed an albedo of 0.21 otherwise (the average value over the Flora family members with known IRAS albedos). Moreover, some thermal parameters had to be specified. The Bond albedo and emissivity were set to 0.1 and 0.9, respectively. The Yarkovsky force sensitively depends on the surface conductivity (K). The conductivity of a surface covered by regolith is low; for Moon, $K = 0.0015$ W/m/K (Rubincam 1995). We choose a slightly lower value, $K = 0.001$ W/m/K, for our experiment. If the surface conductivities of the Flora family asteroids are not orders of magnitude different from this assumed value, the migration speeds modeled in our experiment are correct within a factor of 2.

We neglect collisional disruptions and spin axis reorientations because these events have typical time scales longer than the time span covered by the integration (Farinella *et al*. 1998). Each integrated body thus has a fixed rate and direction of the semimajor axis drift.

Figure 4 shows the evolution of our numerical proper elements, computed as 10-Myr averages of the orbital elements, over 170 Myr. Comparing Fig. 4 with Fig. 2, we notice that the traces left by the individual bodies (in the non-Mars-crossing regime) are not vertical (i.e., keeping constant the proper semimajor axis) but crisscross the proper element space in all directions. This is the result of the combined effects of mean motion resonances and of the Yarkovsky force. As a consequence of the semimajor axis mobility, the bimodality of the diffusion process in resonances observed without the Yarkovsky effect (Fig. 2) is now strongly reduced since bodies move in and out of the resonances. A body migrating towards a resonance is either captured or jumps across (e.g., Bottke *et al*. 2000). The capture probability depends on the rate of the semimajor axis migration and on the resonant width. Small bodies usually migrate faster than large ones and are less frequently captured, but if they are captured, then the responsible resonance is usually large. The capture probability mechanism, though beyond the scope of this work, is worth studying in detail. It is not a pure process of adiabatic capture into resonance, because capture would be possible only in specific directions of migration (outward for jovian resonances and inward for martian resonances), converse to what is observed. In the inner belt, which is dominated by mean motion resonances with Mars, this mechanism becomes complex because these resonances are largely modulated by the secular oscillations of the eccentricity and the perihelion longitude of Mars. The efficiency of the capture mechanism in the mean motion resonances is crucial for obtaining significant mobility in e and i.

The rate at which bodies escape to the Mars-crossing region is about the same as in the experiment without the Yarkovsky force. There are 13 bodies on the Mars-crossing orbits at 120 Myr, and 17 bodies at 170 Myr. This validates our previous finding that the present rate at which the Flora family loses members to the planet-crossing region due to dynamical diffusion in resonances is on the order of 3% every 10^8 years. The overall rate at which the Flora family dynamically evaporates, however, could be better estimated if we could generate a more sophisticated criterion of family membership. This procedure would exclude not only the Mars-crossers but also the bodies whose proper orbital elements significantly depart from the family center (e.g., a case of a body which moves out of the family is that denoted by the label "1" in Fig. 4). At that point, we would need to account for the background population of the inner asteroid belt and then identify the family members at each time step by the hierarchical clustering method of Zappalà *et al*. (1994).

Figure 5 shows the evolution of $\sigma_1(e)$ and $\sigma_1(i)$ computed from the proper elements and Eq. (1). This figure can be directly compared to Fig. 3, where the same quantities are shown for the simulation without the Yarkovsky force. First, it may be noted from Figs. 3 and 5 that the Yarkovsky force somewhat decreases the efficiency of the mean motion resonances in dispersing the Flora family in e. Indeed, with the Yarkovsky force, $\sigma_1(e)$ (Fig. 5a) does not increase as fast in the first 15 Myr as it does in the run without the Yarkovsky force (Fig. 3a). This makes the overall average family dispersion rate in e somewhat smaller. This result may be caused by resonant jumping events, which prevent Flora family members from residing in any single resonance long enough to undergo large secular increases in e. Conversely, $\sigma_1(i)$ in Fig. 5b initially increases faster than in Fig. 2b, and decelerates after 70 Myr. These particular dependencies of σ_1 on t are sensitive to the set of initial conditions and parameters used in the simulation. On the other hand, the average dispersion rates of e and i seen in Fig. 5 are more robust. For this reason, the average dispersion rates are considered for the estimate of the Flora family's age, discussed in the next section.

5. A TENTATIVE ESTIMATE OF THE AGE OF THE FLORA FAMILY

If one can extrapolate the current dynamical dispersion rate of the Flora family in e and i back in time, it may be possible to

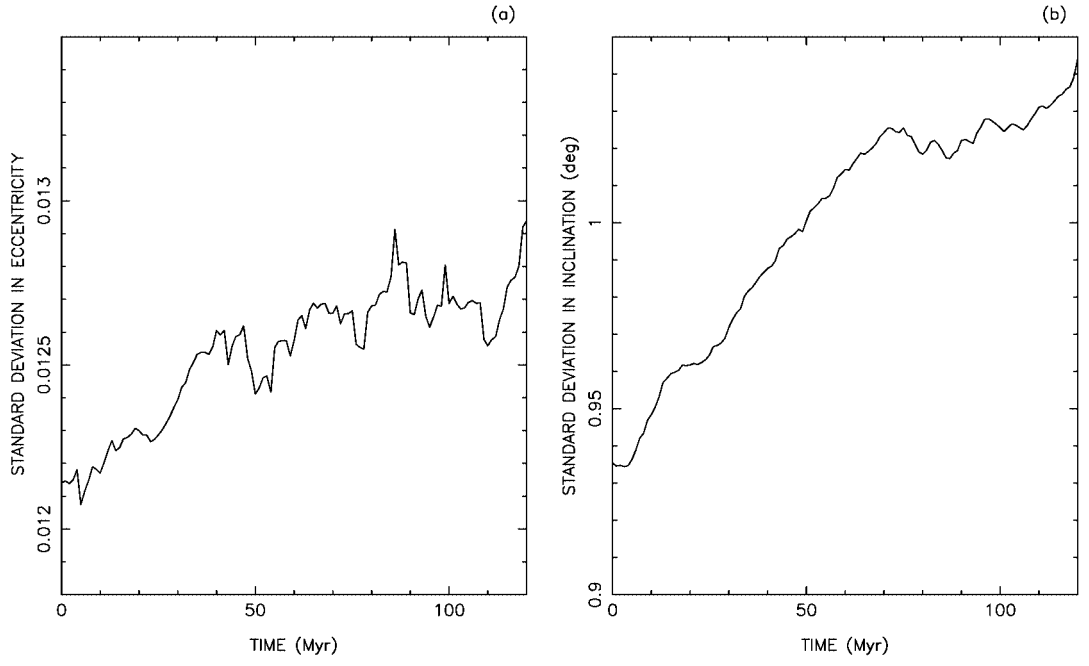

FIG. 5. The same as Fig. 3, but for the run with the Yarkovsky force. $\sigma_1(e)$ (left) increases somewhat slower than in Fig. 3a.

estimate the age of the Flora family. We believe this can be done, with some uncertainty, if two additional assumptions are valid:

(i) We assume that σ_1 is proportional to $C\sqrt{t}$, where C is a constant to be determined. This assumption is motivated by the fact that the chaotic diffusion via narrow mean motion resonances is a random process which can in principle be modeled by the random walk (Murray and Holman 1997). We have verified this assumption on several occasions by numerical simulations of test bodies initially placed on resonant orbits, and by a simple toy model of coupled random walk processes with different characteristics.

(ii) We assume that the ejection velocities were much smaller than those derived from the present dispersion of the Flora family, namely on the order of the escape velocity from the parent body. To simplify further, we approximate the initial orbital distribution in proper e and i by δ-functions, i.e., we assume that after the breakup (assumed to occur at the current family center, see below) the orbits of all ejecta had the same proper eccentricity and proper inclination. This is apparently unrealistic but useful for setting an upper limit on the family age: if the initial orbital dispersion of the family was broader, or if two or more breakups occurred at the Flora family place significantly contributing to its current orbital dispersion, the dynamical diffusion could have created the current family distribution in a shorter time.

The above assumptions facilitate the problem and allow us to grossly estimate the upper limit of the Flora family age by a simple calculation. We denote T as the age of the family; from the observations (i.e., the current standard deviation of the eccentricity distribution), we know that $\sigma_1(e, T) = 0.01214$, and from the numerical simulation (Fig. 5a) we know that $\sigma_1(e, T + 120\ \text{Myr}) = 0.01284$. These two numbers allow us to solve for C and T. We obtain $T \sim 900$ Myr. The same computation, done on the inclination distribution (Fig. 5b) and using $\sigma_1(i, T) = 0.935^\circ$ and $\sigma_1(i, T + 120\ \text{Myr}) = 1.042^\circ$, gives $T \sim 500$ Myr. If instead of using T and $T + 120$ Myr values, linear functions are fit to the curves in Fig. 5, and the age estimates are derived on the basis of the linear functions' increments on 120 Myr, we get ages which differ by less than 10% from the above estimates. Because of the approximations involved in these estimates, we consider the agreement between these two results satisfactory, and we propose that the Flora family is not older than 10^9 years. Future work on this subject can probably characterize the family age better. In a sense, this dating method is complementary to what was done by Milani and Farinella (1994), who suggested a young age for the Veritas family from the characteristic time scale of the chaotic diffusion of (490) Veritas.

Another interesting question is how the shape of the family orbital distribution in proper e and i evolves by dynamical dispersion. This is a difficult subject because ideally we would need to numerically integrate statistically significant samples of bodies over the inferred family age, starting from different initial distributions (i.e., considering the unknown initial distribution of the Flora family as a free parameter of the model). Because this is beyond our current computational ability, we attempt to roughly model the evolution of the Flora family's orbital distribution using a Monte Carlo model.

To build such a model, we assume that the rate of chaotic diffusion is roughly invariant to a small shift of orbital elements. This is essentially true for small changes of e and i, but not for changes in a. In fact, changing the semimajor axis may release a body from a resonance or capture it into a resonance, and its dynamics may largely change. From a statistical point of view, however, we believe that a large ensemble of test bodies with slightly modified semimajor axes would statistically behave the same as the original set. Tests examining the orbital evolution of $D < 20$-km bodies in the inner and central main belt suggest the approximation is valid (Bottke *et al.* 2002).

In the model, we assume that orbital density distributions of the Flora family in e and i at $t = 0$ can be approximated by δ-functions; we initially set $e_j = \langle e \rangle$ and $i_j = \langle i \rangle$, where the index j denotes the simulated 385 bodies and $\langle e \rangle = 0.1459$, $\langle i \rangle = 5.012^\circ$ is the center (computed as the average over the proper elements of the first 385 numbered family members) of the present Flora family. We then proceed by propagating this sample in e and i, assigning to each body one of the relative evolutions[6] of e and i, obtained in our simulation up to $t = 170$ Myr. To extrapolate to larger times, we iterate this procedure.

To grossly account for the complex histories of the individual bodies, the relative e, i evolution of a test body on [0, 170] Myr is assigned to *another*—randomly chosen—body on [170, 340] Myr, and so on. More precisely, when choosing the orbital history of the test body A on the next time interval, we first select the bodies with about the *same* semimajor axis and migration speed as the body A and then randomly choose among them a body B, whose relative e, i evolution is then assigned to A for the next 170 Myr. The same procedure is repeated for every body and every 170-Myr interval. By mixing orbital histories of different bodies, we assume that the Yarkovsky effect has a large efficiency of "smoothing" the resonant chaotic diffusion over the whole sample on time intervals similar to our integration time span (170 Myr).

Before commenting on the results of the above Monte Carlo model, we should consider another issue for the comparison between the simulated and observed family distributions, that is, the family membership identification method. The identification of families in the asteroid belt is usually done by an automatic hierarchical clustering algorithm assuming a metric in the proper orbital elements space and a threshold velocity (Zappalà *et al.* 1994). A body which is separated from the rest of the family members by more than the threshold value is not considered a family member. During the dynamical evolution of the family, some family members either largely diffuse in proper e and i and/or largely drift in semimajor axis, so that at some point they leave the region occupied by the family in proper elements space and thus are no longer identified as family members by the automatic algorithm. To account for this possibility, we need to account for the background population of asteroids in the inner asteroid belt and at each time step run the identification algorithm. Such a procedure is desirable because computations suggest that some of the Flora family members may actually be interlopers (Zappalà *et al.* 1994, Migliorini *et al.* 1995).

Because of the qualitative level of this section, we do not use a sophisticated identification algorithm, but rather specify a simple criterion to judge whether a body is a family member. We eliminate bodies whose proper orbital elements are outside the current borders of the Flora family, which we approximate as a box: $2.12 < a < 2.31$ AU, $0.11 < e < 0.175$, and $3^\circ < i < 7.5^\circ$. Bodies inside the box are considered family members. We are well aware that this assumption introduces an inconsistency in the comparison of the real and simulated orbital distributions, but nevertheless we believe that this simplification is a good starting point.

Figure 6 shows the orbital distributions in e and i computed by the Monte Carlo model. Both distributions closely resemble the

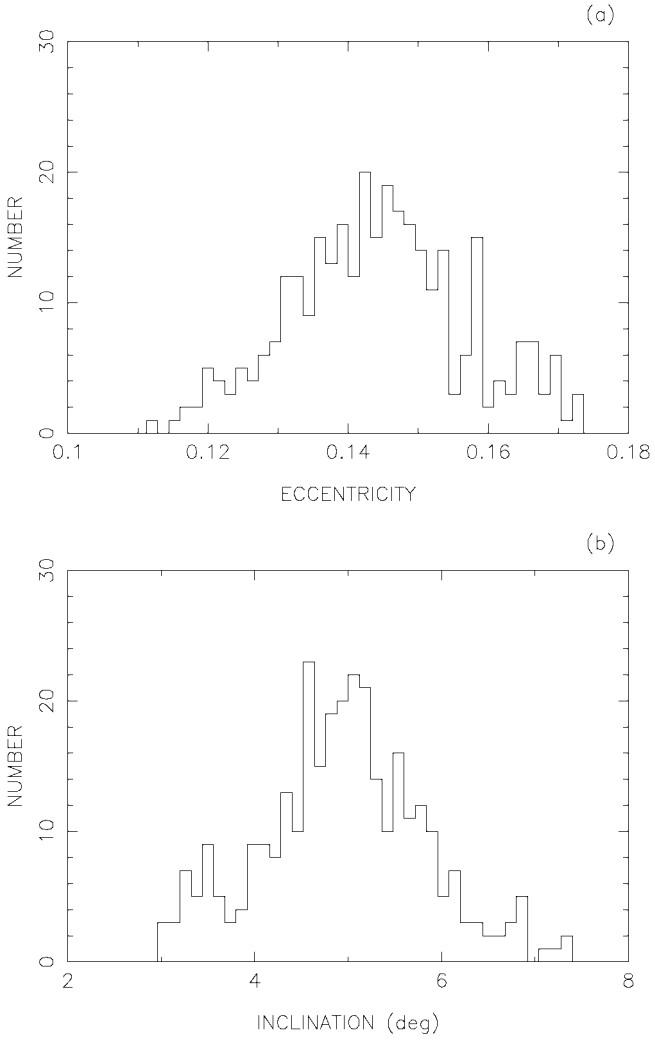

FIG. 6. The orbital distributions in the proper e (a) and the proper i (b) obtained from the Monte Carlo simulation. See text for discussion.

[6] By relative evolution we mean the evolution relative to the initial conditions.

real distributions (compare to Fig. 1). In particular, the simulated distribution in i shows a pyramidal profile that is almost identical to the one in Fig. 1c. The agreement between the eccentricity distributions in Figs. 6a and 1b is a little bit worse but still acceptable. The times for which we have to run the Monte Carlo model in order to get approximately correct values of $\sigma_1(e)$ and $\sigma_1(i)$ are usually between 5×10^8–10^9 years. We can thus conclude that, starting from a very tight grouping, it is possible to obtain the current Flora family distribution in e and i solely by the dynamical effects on 5×10^8–10^9 year time scales. If the grouping was initially more dispersed, or if more than one breakup is responsible for the current family distribution, this event would have occurred significantly more recently than 10^9 years ago.

We have so far avoided the important question of the Flora family dispersion in proper semimajor axis for several reasons. First, the mechanism of dispersing the family in a is different (Yarkovsky force) than the one (mean motion resonances) on which we concentrate in this paper. The Yarkovsky force critically depends on several parameters which are poorly known, and it would be appropriate to run several simulations allowing for different values of the parameters within the acceptable limits. This will be the subject of a future work. Nevertheless, we have already performed several such tests (Nesvorný *et al.* 2001), and the preliminary results seem to suggest that it is easily possible to obtain the Flora family distribution in a entirely from the Yarkovsky effect over a time consistent with the one needed to disperse the family in e and i by resonant diffusion.

Second, the Flora family is highly asymmetric in proper semimajor axis with respect to the position of (8) Flora ($a =$ 2.2014 AU, $e = 0.1528$, and $i = 5.57^\circ$—see Fig. 1a). This led some authors to discuss the possibility that (8) Flora is actually an interloper (Cellino and Zappalà 1993). Even if this might be the case, it does not solve the problem, because the second largest body of the Flora family, (43) Ariadne, has proper semimajor axis close to that of (8) Flora. In fact, one can see in Fig. 1a that the largest bodies of the Flora family are all localized at a smaller semimajor axis than the family center. This supports a scenario in which the parent body of the Flora family was disrupted at 2.2–2.23 AU. If so, one should generate at 2.2–2.23 AU a plausibly tight grouping, resembling a possible outcome of a collisional breakup, and evolve it dynamically over 10^8–10^9 years. Such simulations are currently in progress and show that the asymmetric position of the largest fragments with respect to the smaller ones is a natural outcome of the dynamics: small bodies drifting fast to a smaller semimajor axis are removed by the resonances and Mars encounters, while those drifting to a larger semimajor axis survive.

We can now finally attempt to draw a reasonably complete and plausible scenario of the Flora family origin: (1) The breakup of the parent body happened somewhere at 2.2–2.23 AU. (2) Depending on the magnitude of ejection velocities, some of the fragments were directly injected to the Mars-crossing region and were removed from the vicinity of the main belt. Other fragments started to evolve in the proper elements space due to mean motion resonances with Mars and Jupiter. (3) In the subsequent $<10^9$ years, $>10\%$ of the original family members exited the region occupied in the proper elements space by the current Flora family and are no longer dynamically recognizable as family members. (4) The family dynamically dispersed during this time and achieved the current orbital distribution characterized by a highly asymmetric form in terms of the location of the largest remnants and the e and i vs a dispersions.

This scenario is highly speculative, but to our knowledge, it is the one which best accounts for the observed Flora family dispersion, assuming that it originated from a single parent-body breakup. We caution that we cannot rule out the possibility that multiple breakups occurred in this region. If so, this work shows that dynamical dispersion was efficient in mixing in the proper elements space the fragments coming from different breakups.

6. LINKS OF THE SUGGESTED SCENARIO WITH THE AVAILABLE PHYSICAL DATA

The fact which may partially support a comparatively young age of the Flora family is the cratering record of (951) Gaspra. This is an S-type asteroid, a member of the Flora family, with a cratering age of about 40% of its collision lifetime, which is 0.5 Gyr with a large uncertainty (Chapman *et al.* 1996). To get these ages, Chapman *et al.* (1996) computed the size distribution of the impacting population from the crater counts, assuming a strength scaling. Greenberg *et al.* (1994), however, argued for a collisional lifetime of about 1 Gyr assuming possibly more accurate scaling derived from hydrocodes. Although these age estimates may be wrong by a factor of a few, they may still indicate that the Flora family is a few hundreds of Myr old, in rough agreement with this work.

A steep cumulative crater diameter distribution on the surface of (951) Gaspra, moreover, suggests a size distribution of impactors that could be expected from the Flora family parent-body breakup. It is not clear, however, why the time-integrated crater size distribution on the surface of (951) Gaspra is dominated by the impactors from the Flora family, for the eccentricity of (951) Gaspra makes it cross half the asteroid belt. The crater distribution could thus rather reflect the time-averaged impactor flux in the "typical" asteroid belt as it probably happens on surfaces of other asteroids imaged by spacecrafts which are more heavily cratered and have comparatively shallower crater distributions than (951) Gaspra. The feeling we have from this is that (951) Gaspra is a young object with an exceptional cratering history, not necessarily determined by the typical background population of small bodies in the asteroid belt. It is our conjecture that the impactor flux from the Flora family may have been important (see Dell'Oro *et al.* 2001).

The observed steep size–frequency distribution of the Flora family members (Cellino *et al.* 1991) provides additional clues about the young age of this region. The asteroid families are known to be formed with steep size–frequency distributions which then relax by secondary fragmentations. There is a clear signature of this process for families >1 Gyr in age (Marzari *et al.* 1995, 1999). Hence, it may be argud that the population

in the Flora region is too young (probably <1 Gyr) to have developed a more shallow size–frequency distribution.

Additional evidence of a recent breakup event of a large body in the asteroid belt comes from the high abundance of heavily shocked and degassed L chondrites with ^{40}Ar-^{39}Ar ages around 5×10^8 years. The analysis seems to indicate that the L chondrite parent body suffered a major impact 5×10^8 years ago (Haack *et al*. 1996). Moreover, it was inferred from the thermal evolution of impact-heated rocks after the 0.5-Gyr event and from the high abundance of heavily shocked L chondrites that the parent body was catastrophically disrupted. The L chondrites are the most common group of meteorites with a relative fall frequency of 38%. The average shock level is higher for L chondrites than for other types of chondrites. The recorded shock levels are most likely the result of a single major impact rather than an accumulated effect acquired through numerous impacts over time. The slow cooling rates seem to require an original parent body more than 100 km in diameter.

One may then be tempted to associate the parent body of L chondrites with the parent body of the Flora family. This conjecture is plausible: (1) Dynamically, the Flora family is in the inner asteroid belt which is known to be a dominating source of planet-crossers (Migliorini *et al*. 1998, Morbidelli and Gladman 1998, Morbidelli and Nesvorný 1999). (2) Compositionally, S-type asteroids are thought to be similar to chondrite meteorites (even if space weathering makes their surfaces spectroscopically distinct—Chapman 1996). (3) Chronologically, there is a rough correspondence between the breakup time derived from L chondrites (0.5 Gyr) and the time scale of the dynamical dispersion of the Flora family derived in this paper (0.5–1 Gyr starting from δ-distributions, probably consistent with 0.5 Gyr if an initial moderate dispersion of the family is assumed). More sophisticated studies of the dynamical dispersion process will hopefully allow us to constrain the age of the Flora family better and reinforce (or weaken) this hypothesis.

The constraint which should be met by a plausible scenario of the L chondrites' origin is the observed distribution of their cosmic-ray exposure (CRE) ages (Marti and Graf 1992). The measured CRE ages suggest that most L chondrites spend $\gtrsim 10^7$ years in space being unshielded from cosmic rays (buried less than about 1.5 m in depth in the precursor body) before they impact the Earth. Vokrouhlický and Farinella (2000) modeled the delivery of meteorites to the Earth from the Flora family source region via the Yarkovsky effect (accounting for the cascade of collisional disruptions) and showed that the observed CRE ages are about the ones expected in this scenario in a steady state. This does not exclude other parts of the inner asteroid belt as possible source regions of the L chondrites but is consistent with our suggestion that the Flora family might be a dominating source.

Other observational evidence which may be related to the Flora family breakup documented in the literature is the fossil chondrite meteorites with terrestrial ages ~460–480 Myr (Thorslund and Wickman 1981, Schmitz *et al*. 1997). Schmitz *et al*. (1997) suggest that the accretion rates of meteorites in the Early Ordovician period (~480 Myr ago) were one to two orders of magnitude higher than at present. Moreover, the isotope analysis of the whole-rock limestone layer in which the meteorites were found shows an iridium enrichment, which is plausible with an enhancement of one order of magnitude in the influx rate of cosmic dust. Both findings may reflect a breakup of a meteorite parent body in the asteroid belt by which a large number of bodies was deposited on unstable orbits (either Mars-crossing or in main resonances) and later evolved, in $\approx 10^7$ years, to the Earth-crossing orbits. Additionally, it is possible that impacts on the Moon increased in the past 0.4 Gyr by a factor of a few with respect to earlier epochs (from ^{40}Ar-^{39}Ar dating of lunar spherules—Culler *et al*. 2000 and references therein). The possibility that the catastrophic breakups in the asteroid belt can temporarily enhance the cratering rates of the terrestrial planets and their moons' surfaces has been suggested by Zappalà *et al*. (1998).

If the Flora family is young (~0.5 Gyr), the near-Earth asteroid (433) Eros probably cannot be collisionally related with its parent body, because the surface of (433) Eros imaged by NEAR suggests a $>10^9$ year cratering age (Veverka *et al*. 2000). As (433) Eros is one of the two largest asteroids on near-Earth orbits ((1036) Ganymed is the largest), this raises the question of whether the Flora family may provide most L chondrites but be a less important source of large near-Earth asteroids (NEAs). Large NEAs are thought to leak from the inner asteroid belt by the effect of narrow mean motion resonances with Mars and Jupiter (Migliorini *et al*. 1998, Morbidelli and Nesvorný 1999). Such a process should basically sample the multikilometer bodies in the inner main belt having small perihelion distances. Although the Flora family represents an important component of this population, (433) Eros could have leaked from the inner main belt without being necessarily derived from the family's parent body. Because of its steep size distribution, the Flora family is probably a more important component of the inner main belt population at smaller sizes. Thus, the existence of (433) Eros with old surface on near-Earth orbit is not in apparent contradiction to the suggested link between L chondrites and the Flora family.

Our work suggests that many Flora family members probably evolved to the inner Solar System quite recently. If so, there can be an important subpopulation among the current NEAs with the same spectral properties as the ones observed among the Flora family members. While this is in general terms observed (most NEAs are S-type like (8) Flora), we believe that future spectral observations may even provide some additional clues about the link between the Flora family and some of the small bodies on planet-crossing orbits.

7. PERSPECTIVES

The dynamical dispersion of the Flora family investigated in this work is very probably not a specific aspect of the inner asteroid belt dynamics but should also affect families in other parts of the main belt. From Morbidelli and Nesvorný (1999—Fig. 1),

we can guess that the families largely affected by chaotic diffusion are those in the outer part of the asteroid belt ($2.85 < a < 3.25$ AU). A larger dispersion is expected because the density of narrow mean motion resonances increases approaching Jupiter. A particularly interesting case seems to be the Themis family, which is located at $3.08 < a < 3.23$ AU, $e \sim 0.15$. Resonances in this region are dense (Nesvorný and Morbidelli 1998). The prominent mean motion resonances which delimit the family in semimajor axis are the 11/5 & 3J-2S-1 jovian and three-body resonances at ~3.08 AU and the large 2/1 resonance with Jupiter. The age of the Themis family estimated from the size distribution by Marzari *et al*. (1995) is on order of 2 Gyr. From our simulations of the Flora family and also from a simulation of several resonant bodies in the Themis region, we guess that the effect of resonant diffusion on the Themis family structure over such a long time interval might have been large. The first signature of this effect is probably the existence of several sizable Themis family members in the 5J-2S-2 resonance, which are dispersed over a larger range in the proper e than the other, similarly sized but nonresonant bodies (Morbidelli 2000). Quantifying the dynamical dispersion of the Themis family, and also the other families in the asteroid belt, is an exciting subject for future research.

Recently, the dynamical evolution of the Koronis family was quantified by Bottke *et al*. (2001). The Koronis family, being located at small eccentricities ($e \sim 0.05$) where mean motion resonances are narrow, was not expected to significantly evolve in e and i. It turned out, however, that the Koronis family is intersected by a large number of secular resonances.[7] The simulation showed that the family members drifting in a by the Yarkovsky effect are pushed to the location of the secular resonances, either becoming captured or jumping over them. This interaction between the Yarkovsky effect and secular resonances creates unique structures in proper a, e. These structures, hardly reproducible by alternate means, clearly exist in the observed orbital distribution of nominal members of the Koronis family (Bottke *et al*. 2001). This fact, turning the argument around, is a spectacular proof of the footprints left by the Yarkovsky effect on one of the most prominent asteroid families.

APPENDIX: THE SEMIMAJOR AXIS MOBILITY DUE TO ENCOUNTERS WITH LARGE ASTEROIDS

Contrary to the semimajor axis mobility produced by the Yarkovsky force, which has been a subject of many studies, the longterm effect of large asteroids on the smaller asteroids' evolution was not investigated in detail (except by J. G. Williams, Personal Communication, 1992; see Milani and Knežević 1992, page 223). To quantify this effect, we have selected 300 numbered asteroids (see below) and run a numerical integration assuming them to be massless particles evolving in the gravitational field of seven planets (Venus to Neptune) and the three largest asteroids ((1) Ceres, (2) Pallas, and (4) Vesta). The masses of these three asteroids were assumed to be 4.39×10^{-10}, 1.59×10^{-10}, and 1.69×10^{-10}, respectively, in Sun mass units, according to the determination of Hilton (1999). Other sources (Michalak 2000, Goffin 2001) assign a larger mass to (1) Ceres and smaller masses to (2) Pallas and (4) Vesta.

The 300 asteroids were chosen as the first numbered asteroids which satisfied the following conditions: (1) number designation larger than 4; (2) $2.1 < a < 2.8$ AU (to avoid the proximity to the 2/1 mean motion resonances with Jupiter); (3) $1.85 < q < 2.6$ AU, where q is the perihelion distance (no Mars-crossers); and (4) $i < 15$ deg (to avoid secular resonances at large i).

Our selection process had several goals: (a) we wanted to find bodies that intersected the orbit of at least one of our three massive asteroids; (b) we intended to avoid asteroids which might escape to planet-crossing orbits; and (c) we hoped to minimize the effects of the large mean motion and secular resonances on our sample, because they might potentially hide the expected tiny effects of encounters with the massive asteroids. The advantage in working with real asteroids is that dynamical selection processes over the age of the Solar System remove bodies on unstable trajectories. Hence, large asteroids (i.e., the ones with low designation numbers) should be survivors which reside on stable orbits. In addition, these objects provide a roughly uniform sampling of the main belt, so that the results of the integration represent a sort of "averaged" effect over the belt. The selection criteria excluded more than 50% of the asteroids in the catalogue (mostly due to item 2) so that the object with the highest number which entered our integrated sample is (675) Ludmilla.

We used the *Mercury* integrator of Chambers (1999). This code is based on the symplectic algorithm of Wisdom and Holman (1991), but unlike *Swift* (Levison and Duncan 1994), it symplectically integrates the close encounters between a massless particle and a massive body. Because the close encounter routine is crucial for our needs, we have submitted *Mercury* to a number of tests. The basic test consisted of integrating a system of three bodies: the Sun, a Ceres-mass perturber on a circular orbit, and a massless particle for 10^7 years using a 7.5-day time step, and checking the conservation of the Jacobi constant. Typically, the *Mercury* integrator preserved the Jacobi constant two orders of magnitude better than *Swift* and was thus our best available choice.

The main integration covered 100 Myr using a 7.5-day time step. Only one object ((110) Lydia) had a lifetime less than 100 Myr and was removed before the integration ended. Four objects ((156) Xanthippe, (313) Chaldaea, (405) Thia, and (453) Tea) reached Mars-crossing status ($q < 1.665$ AU) but survived the length of integration. Apart from these particular cases, many other objects (40%) significantly diffused in eccentricity ($|e(100\,\mathrm{Myr}) - e(0)| > 0.002$) due to narrow mean motion resonances, as shown in Fig. 7. This figure—which also plots

[7] The secular resonances are commensurabilities between perihelion and nodal frequencies of asteroids and the proper secular frequencies of planets (see, e.g., Milani and Knežević 1994).

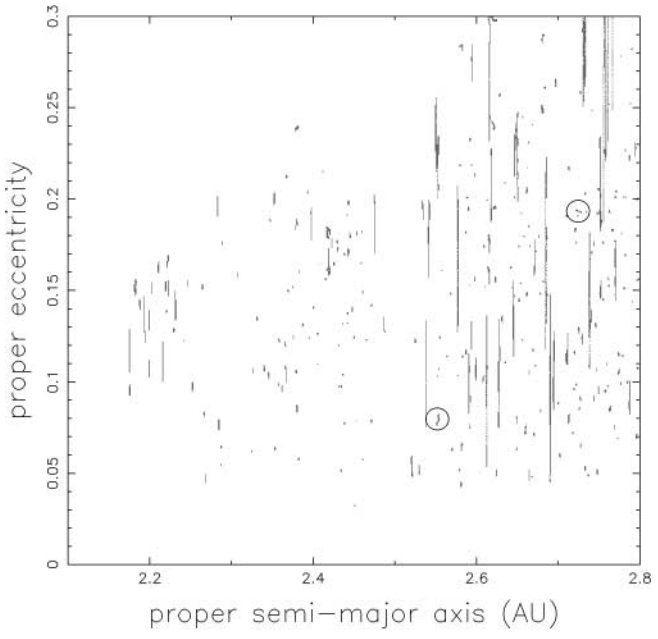

FIG. 7. The evolution of the proper semimajor axis vs proper eccentricity of 300 numbered asteroids taking into account the gravitational perturbations of (1) Ceres, (2) Pallas, and (4) Vesta. The scale of the plot does not permit a clear view of the tiny effects these large asteroids had on the semimajor axis of the simulated bodies. In some cases, the semimajor axis evolution may be noticed (e.g., trails marked by circles). Most evolutions seen in this figure are the proper eccentricity changes due to the chaotic diffusion in the mean motion resonances.

the evolution of the proper semimajor axis and proper eccentricity obtained by averaging the orbital elements over a 10-Myr running window—can be considered as an extension of Fig. 2 to the entire asteroid belt. In the outer belt ($a > 2.5$ AU), the asteroids diffuse in proper eccentricity more than the asteroids in the inner belt ($a < 2.5$ AU), where diffusion is important only in the vicinity of the Flora region ($a \sim 2.2$ AU). The magnitude of chaotic diffusion in the different parts of the asteroid belt is correlated with the density of narrow mean motion resonances (Nesvorný and Morbidelli 1998).

To quantitatively characterize the changes in proper orbital elements, we compute $da_j = a_j(t) - a_j(0)$, $de_j = e_j(t) - e_j(0)$, and $di_j = i_j(t) - i_j(0)$ for each body. The standard deviation over the sample of orbits is then defined as

$$\sigma_2(x;t) = \sqrt{\frac{\sum_j [dx_j]^2}{N-1}}, \qquad \text{(A1)}$$

where x stands for proper a, e, or i, $1 \le j \le N$, and $N = 295$. At $t = 100$ Myr, this results in $\sigma_2(e) = 0.0096$. For $a > 2.5$ AU, we get $\sigma_2(e) = 0.011$. We do not have data beyond 2.8 AU, but from previous studies we may guess that $\sigma_2(e)$ is even larger there. For the inclination, the situation is similar: $\sigma_2(i)$ computed at $2.1 < a < 2.8$ AU is 0.0035 rad per 100 Myr, and somewhat larger at $a > 2.5$ AU. This makes us believe that the dynamical dispersion over time of the eccentricity and inclination is not a specific aspect of dynamical processes governing the Flora family, but it should also be important for the families with $a > 2.5$ AU.

The main motivation for this experiment was to determine the effect of massive asteroids on semimajor axis mobility. Changes in proper a are difficult to see in Fig. 7 because the scale is too large. They are, however, far from negligible. For example, notice the trails left by the two bodies which are surrounded by the circles. These are clear cases of significant proper semimajor axis evolution spanning almost 0.01 AU.

Figure 8a shows the differential and Fig. 8b the cumulative distribution of da at 100 Myr for all integrated bodies except the five Mars-crossers and those with $\max(de) > 0.05$, where $\max(de)$ is the maximum of de computed over the 100-Myr interval. By this last criterion, we eliminate bodies which significantly evolved in the resonances, because their proper semimajor axis could have changed by the effect of resonances (which become large and may overlap at large e). Additionally, we have done two tests to be sure that the measured da is really due to the effect of massive asteroids. In the first test, we correlated the "jumps" in proper semimajor axis with the close encounters with one of the three massive asteroids. As expected, most of the semimajor axis evolutions result from close encounters with (1) Ceres. Second, we have integrated a test sample considering only seven planets as gravitationally active bodies (switching off the perturbations exerted by the massive asteroids). As expected, all bodies had negligible da at 100 Myr in this case.

The distribution in Fig. 8a is not Gaussian-like because of the peak at $da \sim 0.0005$ AU. At 100 Myr, $\sigma_2(a)$ is 0.000835 AU. By least-square fit we have computed that $\sigma_2(a)$ grows with time as $t^{0.63}$. It therefore grows slower than linearly but faster than $\sqrt{t}$. This should not be too much of a surprise, because encounters do not necessarily produce a true random walk in semimajor axis. One must also account for factors like encounters with repeated geometry, asymmetries in the perturbations, etc. Extrapolating this law on 2 Gyr, we get $\sigma_2(a) = 0.0055$ AU, and on 4 Gyr we get $\sigma_2(a) = 0.0085$ AU. The latter value, translated in terms of velocities in the Flora family region, would correspond to an ejection velocity of some 50–60 m/s. Note, however, that the collisional lifetime of the bodies of sizes typically observed in the Flora region (6–9 km in diameter, Fig. 1d) is probably less than a few Gyr (Farinella and Vokrouhlický 1999). Consequently, the above extrapolations make sense only for the largest members of the Flora family.

The effect of massive asteroids on semimajor axis is larger at $a > 2.5$ AU, probably because of the higher frequency and lower mutual velocities of encounters. Computing $\sigma_2(a)$ over the subsample of asteroids with $a > 2.5$ AU, we obtain $\sigma_2(a) = 0.000974$ AU on 100 Myr. Moreover, in this case, $\sigma_2(a;t) \propto t^{0.68}$. This gives $\sigma_2(a) = 0.0119$ AU on 4 Gyr. We note that the above extrapolations to time intervals exceeding the integration time span are very uncertain. Nevertheless, these

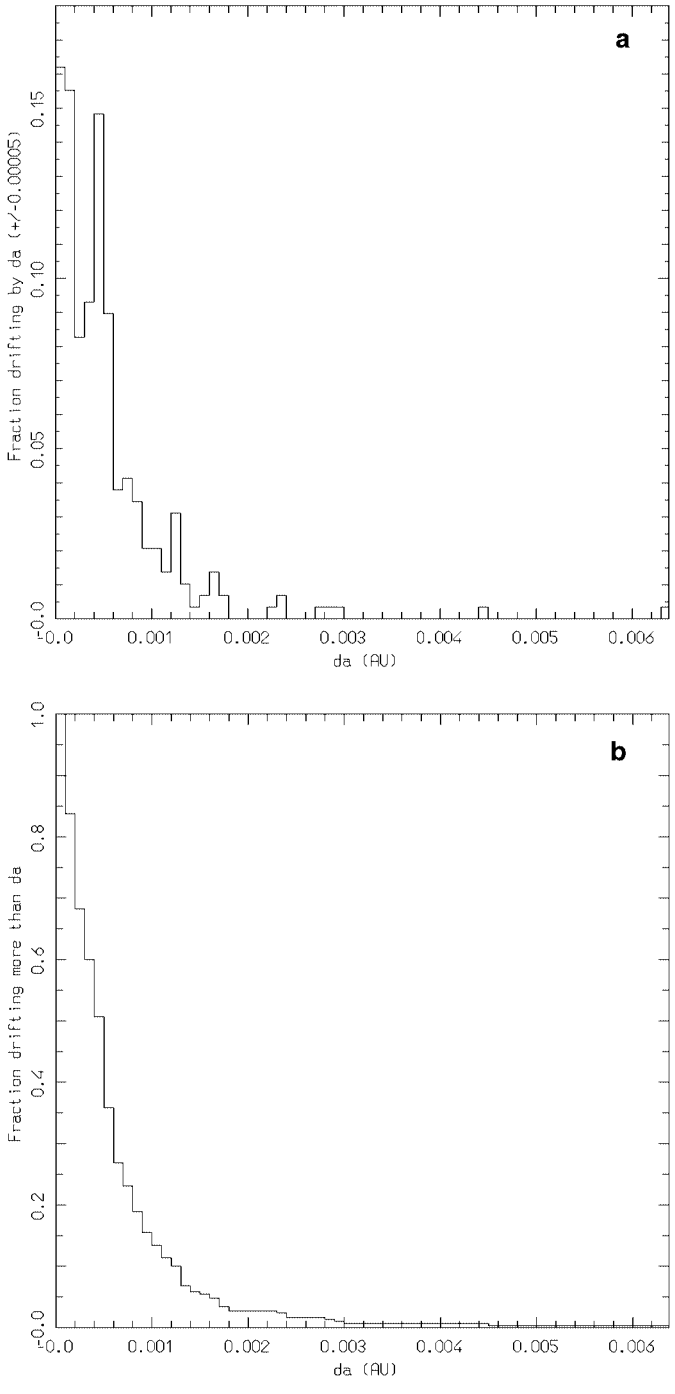

FIG. 8. The differential (a) and cumulative (b) distributions of the evolutions of the proper semimajor axis (*da*—see text) on 100 Myr for 300 numbered asteroids on which we tested the gravitational effect of (1) Ceres, (2) Pallas, and (4) Vesta. Such evolutions do not occur when the gravitational perturbation of large asteroids is neglected.

numbers provide some insight into the magnitude of semimajor axis mobility due to massive asteroids over several Gyr.

The cumulative distribution of Fig. 8b shows that 50% of bodies drifted more than 5×10^{-4} AU over 100 Myr, 10% of bodies drifted more than 0.001 AU over 100 Myr and some 2–3% spanned more than 0.002 AU over 100 Myr. This result implies that massive asteroids force a large fraction of the main belt asteroids to randomly evolve in proper semimajor axis. The magnitude of these evolutions is not large. In the specific case of the Flora family, which our analysis suggests to be $<10^9$ years old and which is predominantly composed of small objects, these evolutions may be safely neglected. Our experiments suggest that the Yarkovsky effect typically provides a dominating source of mobility in a.

ACKNOWLEDGMENTS

The first author (D.N.) acknowledges the financial support of CNRS in the framework of the Poincaré postdoctoral fellowship. We thank A. Cellino and Z. Knežević for their helpful referee reports.

REFERENCES

Benz, W., and E. Asphaug 1999. Catastrophic disruptions revisited. *Icarus* **142**, 5–20.

Binzel, R. P., P. Farinella, V. Zappalà, and A. Cellino 1989. Asteroid rotation rates—distributions and statistics. In *Asteroids II* (R. P. Binzel, T. Gehrels, and M. S. Matthews, Eds.), pp. 416–441. Univ. of Arizona Press, Tuscon.

Bottke, W. F., M. C. Nolan, R. Greenberg, and R. A. Kolvoord 1994. Velocity distributions among colliding asteroids. *Icarus* **107**, 255–268.

Bottke, W. F., D. P. Rubincam, and J. A. Burns 2000. Dynamical evolution of main belt meteoroids: Numerical simulation incorporating planetary perturbations and Yarkovsky thermal forces. *Icarus* **145**, 301–331.

Bottke, W. F., D. Vokrouhlický, M. Brož, D. Nesvorný, and A. Morbidelli 2001. Dynamical spreading of asteroid families via the Yarkovsky effect. *Science* **294**, 1693–1696.

Bottke, W. F., A. Morbidelli, R. Jedicke, J.-M. Petit, H. Levison, P. Michel, T. S. Metcalfe, and B. Gladman 2002. Debiased orbital and size distributions of the near-Earth objects. *Icarus*, in press.

Bowell, E., K. Muinonen, and L. H. Wasserman 1994. A public-domain asteroid orbit database. In *Asteroids, Comets, Meteors* (A. Milani, M. Di Martino, and A. Cellino, Eds.), pp. 477–481. Kluwer, Dordrecht.

Burns, J. A., P. L. Lamy, and S. Soter 1979. Radiation forces on small particles in the Solar System. *Icarus* **40**, 1–48.

Cellino, A., and V. Zappalà 1993. Asteroid "clans": Super-families or multiple events? *Celest. Mech.* **57**, 37–47.

Cellino, A., V. Zappalà, and P. Farinella 1991. The size distribution of main-belt asteroids from IRAS data. *Mon. Not. R. Astron. Soc.* **253**, 561–574.

Cellino, A., P. Michel, P. Tanga, V. Zappalà, P. Paolicchi, and A. Dell'Oro 1999. The velocity–size relationship for members of asteroid families and implications for the physics of catastrophic collisions. *Icarus* **141**, 79–95.

Chambers, J. E. 1999. A hybrid symplectic integrator that permits close encounters between massive bodies. *Mon. Not. R. Astron. Soc.* **304**, 793–799.

Chapman, C. R. 1996. S-type asteroids, ordinary chondrites, and space weathering: The evidence from Galileo's fly-bys of Gaspra and Ida. *Meteoritics* **31**, 699–725.

Chapman, C. R., J. Veverka, M. Belton, G. Neukum, and D. Morrison 1996. Cratering on Gaspra. *Icarus* **120**, 231–245.

Culler, T. S., T. A. Becker, R. A. Muller, and P. R. Renne 2000. Lunar impact history from ^{40}Ar/^{39}Ar dating of glass spherules. *Science* **287**, 1785–1788.

Dell'Oro, A., P. Paolicchi, A. Cellino, V. Zapralà, P. Tanga, and P. Michel 2001. The role of families in determining collision probability in the asteroid main belt. *Icarus* **153**, 52–60.

Farinella, P., and D. R. Davis 1992. Collision rates and impact velocities in the Main Asteroid Belt. *Icarus* **97**, 111–123.

Farinella, P., and D. Vokrouhlický 1999. Semimajor axis mobility of asteroidal fragments. *Science* **283**, 1507–1510.

Farinella, P., D. Vokrouhlický, and W. K. Hartmann 1998. Meteorite delivery via Yarkovsky orbital drift. *Icarus* **132**, 378–387.

Fujiwara, A., P. Cerroni, D. R. Davis, E. Ryan, M. DiMartino, K. Holsapple, and K. Housen 1989. Experiments and scaling laws on catastrophic collisions. In *Asteroids II* (R. P. Binzel, T. Gehrels, and M. S. Matthews, Eds.), pp. 240–265. Univ. of Arizona Press, Tuscon.

Gladman, B. J., F. Migliorini, A. Morbidelli, V. Zappalà, P. Michel, A. Cellino, C. Froeschlé, H. F. Levison, M. Bailey, and M. Duncan 1997. Dynamical lifetimes of objects injected into asteroid belt resonances. *Science* **277**, 197–201.

Goffin, E. 2001. New determination of the mass of Pallas. *Astron. Astrophys.* **365**, 627–630.

Greenberg, R., M. C. Nolan, W. F. Bottke, R. A. Kolvoord, and J. Veverka 1994. Collisional history of Gaspra. *Icarus* **107**, 84–97.

Greenberg, R., W. F. Bottke, M. Nolan, P. Geissler, J.-M. Petit, D. Durda, E. Asphaug, and J. Head 1996. Collisional and dynamical history of Ida. *Icarus* **120**, 106–118.

Haack, H., P. Farinella, E. Scott, and K. Keil 1996. Meteoritic, asteroidal, and theoretical constraints on the 500-Ma disruption of the L chondrite parent body. *Icarus* **119**, 182–191.

Hartmann, W. K., P. Farinella, D. Vokrouhlický, S. J. Weidenschilling, A. Morbidelli, F. Marzari, D. Davis, and E. Ryan 1999. Reviewing the Yarkovsky effects: New light on the delivery of stone and iron meteorites from the asteroid belt. *Meteoritics Planet. Sci.* **34**A, 161–168.

Henrard, J. 1982. Capture into resonance—an extension of the use of adiabatic invariants. *Celest. Mech.* **27**, 3–22.

Hilton, J. L. 1999. US Naval Observatory ephemerides of the largest asteroids. *Astron. J.* **117**, 1077–1086.

Knežević, Z., C. Froeschlé, A. Lemaître, A. Milani, and A. Morbidelli 1995. Comparison between two theories of asteroid proper elements. *Astron. Astrophys.* **293**, 605–612.

Levison, H. F., and M. Duncan 1994. The longterm behavior of short-period comets. *Icarus* **108**, 18–36.

Love, S. G., and T. J. Ahrens 1996. Catastrophic impacts on gravity-dominated asteroids. *Icarus* **124**, 141–155.

Martelli, G., E. V. Ryan, A. M. Nakamura, and I. Giblin 1994. Catastrophic disruption experiments: Recent results. *Planet. Space Sci.* **42**, 1013–1026.

Marti, K., and T. Graf 1992. Cosmic-ray exposure history of ordinary chondrites. *Annu. Rev. Earth Planet. Sci.* **20**, 221–243.

Marzari, F., D. Davis, and V. Vanzani 1995. Collisional evolution of asteroid families. *Icarus* **113**, 168–187.

Marzari, F., P. Farinella, and D. R. Davis 1999. Origin, aging, and death of asteroid families. *Icarus* **142**, 63–77.

Melosh, H. J. 1989. *Impact Cratering: A Geologic Process*. Oxford Univ. Press, New York.

Michalak, G. 2000. Determination of asteroid masses—I. (1) Ceres, (2) Pallas and (4) Vesta. *Astron. Astrophys.* **360**, 363–374.

Michel, P., W. Benz, P. Tanga, and D. C. Richardson 2001. New simulations of collisions between asteroids in the gravity regime: Comparison with the properties of some observed asteroid families. In *Asteroids 2001, from Piazzi to the 3rd Millennium, June 11–15, 2001*, Palermo, Italy.

Migliorini, F., V. Zappalà, R. Vio, and A. Cellino 1995. Interlopers within asteroid families. *Icarus* **118**, 271–291.

Migliorini, F., P. Michel, A. Morbidelli, D. Nesvorný, and V. Zappalà 1998. Origin of Earth-crossing asteroids: A quantitative simulation. *Science* **281**, 2022–2024.

Milani, A., and P. Farinella 1994. The age of the Veritas asteroid family deduced by chaotic chronology. *Nature* **370**, 40–41.

Milani, A., and Z. Knežević 1990. Secular perturbation theory and computation of asteroid proper elements. *Celest. Mech. Dyn. Astron.* **49**, 347–411.

Milani, A., and Z. Knežević 1992. Asteroid proper elements and secular resonances. *Icarus* **98**, 211–232.

Milani, A., and Z. Knežević 1994. Asteroid proper elements and the dynamical structure of the asteroid main belt. *Icarus* **107**, 219–254.

Morbidelli, A. 2000. Asteroids: Living in the kingdom of chaos. *Bull. Am. Astron. Soc.* **32**, 05.01 (abstract).

Morbidelli, A. 2002. *Modern Celestial Mechanics. Aspects of the Solar System Dynamics. Gordon and Breach*, New York, in press.

Morbidelli, A., and B. Gladman 1998. Orbital and temporal distributions of meteorites originating in the asteroid belt. *Meteoritics Planet. Sci.* **33**, 999–1016.

Morbidelli, A., and D. Nesvorný 1999. Numerous weak resonances drive asteroids toward terrestrial planets orbits. *Icarus* **139**, 295–308.

Morbidelli, A., V. Zappalà, M. Moons, A. Cellino, and R. Gonzi 1995. Asteroid families close to mean motion resonances: Dynamical effects and physical implications. *Icarus* **118**, 132–154.

Murray, N., and M. Holman 1997. Diffusive chaos in the outer asteroid belt. *Astron. J.* **114**, 1246–1259.

Nesvorný, D., and A. Morbidelli 1998. Three-body mean motion resonances and the chotic structure of the asteroid belt. *Astron. J.* **116**, 3029–3037.

Nesvorný, D., and A. Morbidelli 1999. An analytic model of three-body mean motion resonances. *Celest. Mech. Dyn. Astron.* **71**, 243–271.

Nesvorný, D., A. Morbidelli, D. Vokrouhlický, W. F. Bottke, and M. Brož 2001. The Flora family: A case of the dynamically dispersed collisional swarm? In *Asteroids 2001, from Piazzi to the 3rd Millennium, June 11–15, 2001*, Palermo, Italy.

Öpik, E. J. 1951. Collision probabilities with the planets and the distribution of interplanetary matter. *Proc. R. Irish Acad.* **54**, 165–199.

Petit, J.-M., and P. Farinella 1993. Modelling the outcomes of high-velocity impacts between small Solar System bodies. *Celest. Mech.* **57**, 1–28.

Pisani, E., A. Dell'Oro, and P. Paolicchi 1999. Puzzling asteroid families. *Icarus* **142**, 78–88.

Rubincam, D. P. 1995. Asteroid orbit evolution due to thermal drag. *J. Geophys. Res.* **100**, 1585–1594.

Rubincam, D. P. 1998. Yarkovsky thermal drag on small asteroids and Mars–Earth delivery. *J. Geophys. Res.* **103**, 1725–1732.

Schmitz, B., B. Peucker-Ehrenbrink, M. Lindsröm, and M. Tassinari 1997. Accretion rates of meteorites and cosmic dust in the Early Ordovician. *Science* **278**, 88–90.

Spitale, J., and R. Greenberg 2001. Numerical evaluation of the general Yarkovsky effect: Effects on semimajor axis. *Icarus* **149**, 222–234.

Tanga, P., A. Cellino, P. Michel, V. Zappalà, P. Paolicchi, and A. Dell'Oro 1999. On the size distribution of asteroid families: The role of geometry. *Icarus* **141**, 65–78.

Thomas, P. C., M. J. S. Belton, B. Carcich, C. R. Chapman, M. E. Davies, R. Sullivan, and J. Veverka 1996. The shape of Ida. *Icarus* **120**, 20–32.

Thorslund, P., and F. E. Wickman 1981. Middle Ordovician chondrite in fossiliferous limestone from Brunflo, central Sweden. *Nature* **289**, 285–286.

Veverka, J., M. Robinson, P. Thomas, S. Murchie, J. F. Bell, N. Izenberg, C. Chapman, A. Harch, M. Bell, B. Carcich, A. Cheng, B. Clark, D. Domingue, D. Dunham, R. Farquhar, M. J. Gaffey, E. Hawkins, J. Joseph, R. Kirk, H. Li, P. Lucey, M. Malin, P. Martin, L. McFadden, W. J. Merline, J. K. Miller, W. M. Owen, C. Peterson, L. Prockter, J. Warren, D. Wellnitz, B. G. Williams, and D. K. Yeomans 2000. NEAR at Eros: Imaging and spectral results. *Science* **289**, 2088–2097.

Veverka, J., P. C. Thomas, M. Robinson, S. Murchie, C. Chapman, M. Bell, A. Harch, W. J. Merline, J. F. Bell, B. Bussey, B. Carcich, A. Cheng, B. Clark, D. Domingue, D. Dunham, R. Farquhar, M. J. Gaffey, E. Hawkins, N. Izenberg, J. Joseph, R. Kirk, H. Li, P. Lucey, M. Malin, L. McFadden, J. K. Miller, W. M. Owen, C. Peterson, L. Prockter, J. Warren, D. Wellnitz, B. G. Williams, and D. K. Yeomans 2001. Imaging of small-scale features on 433 Eros from NEAR: Evidence for a complex regolith. *Science* **292**, 484–488.

Vokrouhlický, D. 1998a. Diurnal Yarkovsky effect as a source of mobility of meter-sized asteroidal fragments. I. Linear theory. *Astron. Astrophys.* **335**, 1093–1100.

Vokrouhlický, D. 1998b. Diurnal Yarkovsky effect as a source of mobility of meter-sized asteroidal fragments. II. Non-sphericity effects. *Astron. Astrophys.* **338**, 353–363.

Vokrouhlický, D. 1999. A complete linear model for the Yarkovsky thermal force on spherical asteroid fragments. *Astron. Astrophys.* **344**, 362–366.

Vokrouhlický, D., and P. Farinella 1998. The Yarkovsky seasonal effect on asteroidal fragments: A nonlinearized theory for the plane-parallel case. *Astron. J.* **116**, 2032–2041.

Vokrouhlický, D., and P. Farinella 1999. The Yarkovsky seasonal effect on asteroidal fragments: A nonlinearized theory for spherical bodies. *Astron. J.* **118**, 3049–3060.

Vokrouhlický, D., and P. Farinella 2000. Efficient delivery of meteorites to the Earth from a wide range of asteroid parent bodies. *Nature* **407**, 606–608.

Vokrouhlický, D., M. Brož, P. Farinella, and Z. Knežević 2001. Yarkovsky-driven leakage of Koronis family members: The case of 2953 Vysheslavia. *Icarus* **150**, 78–93.

Wisdom, J., and M. Holman 1991. Symplectic maps for the N-body problem. *Astron. J.* **102**, 1528–1538.

Yeomans, D. K., P. G. Antreasian, J.-P. Barriot, S. R. Chesley, D. W. Dunham, R. W. Farquhar, J. D. Giorgini, C. E. Helfrich, A. S. Konopliv, J. V. McAdams, J. K. Miller, W. M. Owen, Jr., D. J. Scheeres, P. C. Thomas, J. Veverka, and B. G. Williams 2000. Radio science results during the NEAR–Shoemaker Spacecraft rendezvous with Eros. *Science* **289**, 2085–2088.

Zappalà, V., A. Cellino, P. Farinella, and A. Milani 1994. Asteroid families. II. Extension to unnumbered multiopposition asteroids. *Astron. J.* **107**, 772–801.

Zappalà, V., A. Cellino, A. Dell'Oro, F. Migliorini, and P. Paolicchi 1996. Reconstructing the original ejection velocity fields of asteroid families. *Icarus* **124**, 156–180.

Zappalà, V., A. Cellino, B. J. Gladman, S. Manley, and F. Migliorini 1998. NOTE: Asteroid showers on Earth after family breakup events. *Icarus* **134**, 176–179.